

Thermal Conductivity of Nine Polyatomic Gases at Low Density

F. J. Uribe

Department of Physics, Universidad Autonoma Metropolitana – Iztapalapa, Mexico, D. F.

E. A. Mason and J. Kestin

Brown University, Providence, RI 02912

Received October 18, 1989; revised manuscript received March 28, 1990

We present a complete set of easily programmable computer algorithms, and a set of numerical tables, for the thermal conductivities of the nine gases: N₂, O₂, NO, CO, CO₂, N₂O, CH₄, CF₄, and SF₆. This complements our earlier corresponding-states work on the equilibrium and transport properties of these gases [J. Phys. Chem. Ref. Data 16, 445 (1987); 17, 255 (1988)]. The results embrace the temperature range from $T^* = kT/\epsilon = 1$ up to a nominal upper limit of 3000 K. The accuracy achieved is specified, and the correlation can be used in a predictive mode.

Key words: corresponding states; heat conductivity; polyatomic gases; thermal conductivity.

Contents

1. Introduction	1124	8. Conductivity of carbon tetrafluoride (CF ₄) ..	1130
2. Methodology	1125	9. Conductivity of sulfur hexafluoride (SF ₆)....	1131
3. Functionals and Parameters.....	1125	B1. Universal Constants	1132
4. Experimental Data	1125	B2. Molecular Weights	1132
5. Validation, Deviation Plots, and Accuracy ..	1126	B3. Effective spherical scaling parameters,	1132
6. Description of the Tables	1127	B4. Material parameters for the calculation of D_{rot} and λ	1132
7. Tables	1127	C1. Values of T_{cross}^* for switching from Eq. (C5a) to Eq. (C5b) for $\rho D_{rot}/\eta$	1134
8. Acknowledgments.....	1131		
9. References to Introductory Text	1131		
Appendix A. General Formulas.....	1131		
Appendix B. Material and Physical Constants In- cluding Scaling Factors	1132		
Appendix C. Correlation Equations for Function- als	1133		
Appendix D. Deviation Plots.....	1134		
Appendix E. References for Deviation Plots	1136		

List of Tables

1. Conductivity of nitrogen (N ₂).....	1127
2. Conductivity of oxygen (O ₂).....	1127
3. Conductivity of nitric oxide (NO).....	1128
4. Conductivity of carbon monoxide (CO)....	1128
5. Conductivity of carbon dioxide (CO ₂).....	1129
6. Conductivity of nitrous oxide (N ₂ O)	1129
7. Conductivity of methane (CH ₄)	1130

List of Figures

D1. Deviation plot for the thermal conductivity of N ₂	1134
D2. Deviation plot for the thermal conductivity of O ₂	1134
D3. Deviation plot for the thermal conductivity of NO	1134
D4. Deviation plot for the thermal conductivity of CO	1135
D5. Deviation plot for the thermal conductivity of CO ₂	1135
D6. Deviation plot for the thermal conductivity of N ₂ O	1135
D7. Deviation plot for the thermal conductivity of CH ₄	1135
D8. Deviation plot for the thermal conductivity of CF ₄	1136
D9. Deviation plot for the thermal conductivity of SF ₆	1136
D10. Correlation plot between Prandtl number and rotational collision number	1136

©1990 by the U.S. Secretary of Commerce on behalf of the United States. This copyright is assigned to the American Institute of Physics and the American Chemical Society.

Reprints available from ACS; see Reprints List at back of issue.

List of Symbols

A^*	proportional to $\rho D/\eta$, Eqs. (A4) and (A5); equal to ratio of collision integrals, Eq. (C1)	$\Delta_{\text{ex}}^{\Theta\Theta}$	correction for resonant exchange of molecular rotational energy due to quadrupole-quadrupole interactions
c_v	specific heat at constant volume	ϵ	energy scaling parameter; depth of potential energy well
c_p	specific heat at constant pressure	η	viscosity
C_p	molar heat capacity at constant pressure	κ	thermal diffusivity, Eq. (5)
C_{rot}	molar heat capacity due to molecular rotation	λ	thermal conductivity
C_{vib}	molar heat capacity due to molecular vibration	λ_{tr}	contribution of molecular translational energy to λ , Eqs. (1), (A1), (A2)
C_{elec}	molar heat capacity due to molecular electronic degrees of freedom	λ_{rot}	contribution of molecular rotational energy to λ , Eqs.(1),(A1), (A3)
C_{spin}	constant needed to calculate the temperature dependence of Δ_{spin} , Eq. (A7)	λ_{vib}	contribution of molecular vibrational energy to λ , Eqs.(1),(A1), (A4)
D	self-diffusion coefficient	λ_{elec}	contribution of molecular electronic energy to λ , Eqs.(1),(A1), (A5)
D_{rot}	coefficient for the diffusion of molecular rotational energy	μ	molecular dipole moment
D_{vib}	coefficient for the diffusion of molecular vibrational energy	ρ	mass density of gas
D_{elec}	coefficient for the diffusion of molecular electronic energy	ρ^*	high-temperature distance scaling parameter, Appendix C
E^*	ratio of collision integrals, Eq. (A13)	θ_{rot}	scale factor for molecular rotation, equal to $\hbar^2/2Ik$, where I is the molecular moment of inertia
f_η	higher-order correction factor for viscosity, Eq. (A12)	Θ	molecular quadrupole moment
$g^{\mu\mu}$	temperature-dependent dimensionless factor needed in the calculation of $\Delta_{\text{ex}}^{\mu\mu}$ Eqs. (A8) and (C6a)	σ	distance scaling parameter (used only to calculate η)
$g^{\mu\Theta}$	temperature-dependent dimensionless factor needed in the calculation of $\Delta_{\text{ex}}^{\mu\Theta}$ Eqs. (A9) and (C6b)	$\Omega^{(c,s)*}$	reduced collision integral
$g^{\Theta\Theta}$	temperature-dependent dimensionless factor needed in the calculation of $\Delta_{\text{ex}}^{\Theta\Theta}$ Eqs. (A10) and (C6c)	$\Omega^{(1,1)*}$	reduced collision integral for diffusion
h, \hbar	Planck constant, Table B1	$\Omega^{(2,2)*}$	reduced collision integral for viscosity
k	Boltzmann constant, Table B1		
m	mass of a molecule		
M	molecular weight		
N_A	Avogadro constant, Table B1		
Pr	Prandtl number, Eq. (2)		
R	universal gas constant, Table B1		
T	temperature		
T^*	reduced temperature, kT/ϵ		
V_0	short range energy parameter of intermolecular exponential repulsion		
V_0^*	high-temperature scaling parameter, V_0/ϵ		
Z_{rot}	collision number for rotational relaxation		
Z_{rot}^∞	high-temperature asymptotic value of Z_{rot}		
α	high-temperature parameter, $V_0^*/T^* = V_0/kT$		
Δ_{rot}	correction to λ for interaction of molecular rotational and translational energy, Eqs. (A2), (A3), (A6)		
Δ_{spin}	correction to λ for alignment of molecular angular momentum ("spin polarization"), Eqs. (A2) and (A7)		
$\Delta_{\text{ex}}^{\mu\mu}$	correction for resonant exchange of molecular rotational energy due to dipole-dipole interactions		
$\Delta_{\text{ex}}^{\mu\Theta}$	correction for resonant exchange of molecular rotational energy due to dipole-quadrupole interactions		

1. Introduction

Accurate correlations and predictions of the equilibrium and transport properties of gases and gas mixtures are needed as elements for data bases for the design or optimization of many processes and devices of industrial importance. For low-density gases this need has been partially met for a number of simple gases, thanks to the existence of a highly developed kinetic theory and of a principle of corresponding states for molecular interactions. However, the complexity of the thermal conductivity of molecular gases, and its dependence on molecular internal degrees of freedom and details of inelastic collisions, has thus far prevented its inclusion in any such general correlation scheme.

The situation has recently changed through the development of a correlation that relates the diffusion coefficient for molecular rotational energy to measurable rotational relaxation times.¹ This relation has been validated with respect to accurate data for N_2 , CO , CO_2 , N_2O , CH_4 , and CF_4 .

In this paper we present a complete set of computer algorithms, and a set of numerical tables, for the thermal conductivities of the above-mentioned six gases, plus O_2 , NO , and SF_6 . This work complements our earlier work on the equilibrium and transport properties of eleven polyatomic gases.² The two gases missing are C_2H_4 and C_2H_6 . For these gases the theory is not yet able to cope with the fact that the molecules have several internal degrees of freedom which are readily excited by collisions, and not just a single degree of freedom for rotation that is easily excited.

2. Methodology

The correlation is based on a kinetic theory that treats the contributions of the different molecular degrees of freedom to the thermal conductivity separately. Thus the thermal conductivity, λ , can be written as a sum of contributions from translational, rotational, vibrational, and electronic degrees of freedom,

$$\lambda = \lambda_{tr} + \lambda_{rot} + \lambda_{vib} + \lambda_{elec} \quad (1)$$

To a first, rough approximation these contributions are independent; the translational contribution is like that of a monatomic gas, and the other contributions correspond to the transport of molecular internal energy by diffusion mechanisms. In this first approximation, λ can be calculated from knowledge of the viscosity (η) the self-diffusion coefficient (D), and the specific heat of the gas. A more careful treatment shows that the contributions to λ are not independent, but are modified by inelastic molecular collisions.^{3,4} Each internal degree of freedom then requires its own diffusion coefficient, and there are corrections to each term in Eq. (1) because of interactions with the other degrees of freedom.

In practice, only the translation-rotation interaction is important for the nine gases considered here. The vibrational relaxation times are so long⁵ that the vibrational degrees of freedom can be considered to behave independently. Electronic excitation is significant in the case of NO, but for this gas simplifications occur because the electronic degrees of freedom make only a small contribution to the specific heat and because the electronic relaxation time is nearly ten times longer than the rotational relaxation time.⁶ As a result, the electronic degrees of freedom can also be treated as independent to a good approximation. However, even with all these simplifications, substantial information in addition to η , D , and c_v is now needed to calculate λ : a diffusion coefficient for rotational energy, D_{rot} , a collision number for rotational relaxation, Z_{rot} , and the individual contributions to the specific heat, C_{rot} , C_{vib} , and C_{elec} . All of these quantities are functions of temperature. The specific heats can be obtained by well-established methods of statistical thermodynamics^{7a,b}; the temperature dependence of Z_{rot} is reasonably well-determined from theory,^{8,9} and involves one new parameter, the limiting high-temperature value, Z_{rot}^∞ ; the behavior of D_{rot} is found from that of Z_{rot} ,¹ and it is this relation that makes the present correlation possible. The value of η and of $D \approx D_{vib} \approx D_{elec}$ are available from a previous correlation² which was based largely on a principle of corresponding states.

In summary, the present correlation permits λ to be calculated from known quantities, with the addition of only one new parameter, Z_{rot}^∞ . The value of Z_{rot}^∞ can be obtained, in principle at least, from a single accurate measurement of λ or of Z_{rot} (e.g., from sound absorption). In practice, we have used the best available measurements of both λ and Z_{rot} to determine an optimum value for Z_{rot}^∞ . For O₂ and NO we have relied more on

the relaxation measurements because sufficiently reliable values of λ are not available.

3. Functionals and Parameters

The calculations are most conveniently specified in terms of dimensionless quantities, in particular the group $\rho D/\eta$, where ρ is the mass density, and the group $\lambda M/\eta R$. The latter is related to the Prandtl number, Pr , by

$$Pr = \frac{C_p}{R} \left(\frac{\eta R}{\lambda M} \right), \quad (2)$$

where C_p is the molar heat capacity, R is the universal gas constant, and M is the molecular weight. These dimensionless quantities are calculated from a principle of corresponding states augmented by a somewhat complicated set of formulas given in Appendix A. The necessary constants and parameters are collected in Appendix B, and the functionals appearing in the formulas are in Appendix C. The main functionals are (nearly) universal functions of temperature when written in terms of scale factors representing molecular interaction energy — at low temperatures a scale factor ϵ corresponding to the depth of the potential-energy well, and at high temperatures a scale factor V_0 corresponding to the strength of the intermolecular repulsion as represented by an exponential function. A dimensionless scale factor ρ^* also occurs at the point where the low-temperature and high-temperature expressions for the functionals join at $T^* = kT/\epsilon = 10$. Minor functionals depend on temperature through a scale factor θ_{rot} , which corresponds to the molecular moment of inertia. These minor functionals also depend on such parameters as molecular dipole and quadrupole moments. The complete formulas appear in Appendix A. No scale factor σ corresponding to molecular size or interaction range occurs explicitly in the present calculations; such a scale factor occurs only indirectly through the viscosity η which is already available from an earlier correlation.²

Table B1 contains values of the universal physical constants employed in this work,¹⁰ and Table B2 contains the values of the molecular weights of the gases.¹¹ The energy scaling parameters ϵ , together with the scale factor ρ^* , are listed in Table B3. These are the same values as used previously²; they have been normalized with respect to the following values for argon:

$$\epsilon/k = 141.5 \text{ K}, \quad \sigma = 0.3350 \text{ nm}.$$

The material parameters needed for the calculation of D_{rot} and λ , according to the formulas in Appendix A, are given in Table B4.

4. Experimental Data

The experimental thermal conductivity data considered in this work were contained in over 1000 citations,

based on a computer output supplied to us by the Purdue University Center for Information and Numerical Data Analysis (CINDAS), supplemented with citations from the IUPAC Transport Properties Research Centre at Imperial College, London, and from our own resources. All citations were scrutinized and reduced to about 30 references upon which our comparisons with experiment are ultimately based. The latter were read, critically evaluated, and divided into two classes called primary data (PD) and secondary data (SD).

The division into two classes was based on several objective and subjective criteria. These were: (a) an evaluation of the capability of the method used and of the theory of the instrument; (b) a subjective assessment of the reliability of the data, guided by an examination of internal consistency of error analysis and reproducibility; (c) the authors' statement of precision and accuracy; and (d) a direct intercomparison of results from different laboratories and of results obtained by different methods. In practice, all primary data were obtained by the transient hot-wire method.¹²

The primary data were used essentially as guides to the formulation of the relation between D_{rot} and Z_{rot} that forms the basis of the correlation.¹ Secondary data served for validation and for the inclusion of the gases O_2 and NO . The references listed in the bibliography of Appendix E contain both primary and secondary data.

Similar remarks apply to the various relaxation measurements that were the source of the Z_{rot} values used in the correlation, but here the experimental uncertainties were very much greater than in the case of the thermal conductivity measurements. The final sources appear with Table B4.

5. Validation, Deviation Plots, and Accuracy

Validation of our computational procedures is represented by 9 deviation plots in Appendix D. The class of the data (PD or SD) is indicated in the captions. There are no primary data for O_2 and NO , and direct primary data at only one temperature for SF_6 . Also shown are correlations for N_2 and CO obtained by Millat and Wakeham,¹³ who used a procedure quite similar to the present one but performed a correlation for each system individually. Their procedure yields somewhat greater accuracy in the region where reliable data exist, but is less reliable for prediction (i.e., extrapolation). The agreement between our results and theirs is excellent. Points are also shown for a similar earlier correlation by Millat *et al.*¹⁴ for N_2 , CO , CO_2 , CH_4 , and CF_4 in the temperature range 300–1000 K. Again the agreement is excellent, except for CH_4 at the highest temperatures. Half the discrepancy for CH_4 is due to the use of different specific heats and viscosities.

We have not included comparisons with several important earlier correlations^{15–17} for N_2 , O_2 , and CH_4 , since these are essentially representations of experimental re-

sults that include data we would now regard as secondary.

On the basis of an analysis of the uncertainties in the correlations for Z_{rot} and D_{rot} , and of the comparison with accurate measurements (i.e., the results in Figs. D1–D9), we estimate the uncertainty of the present correlations for λ to be 1.5% in the range 300–500 K, deteriorating to 3% at lower and higher temperatures, for the seven gases N_2 , CO , CO_2 , N_2O , CH_4 , CF_4 , and SF_6 .¹ For O_2 and NO we increase these estimates to 3% in the range 300–500 K, rising to 5% at lower and higher temperatures. For these two gases we believe that our calculated results are more accurate than the existing secondary data, but we cannot guarantee it.

In no case do we recommend the correlation for λ to be used at temperatures lower than $T^* = 1$, where our earlier correlation for the viscosities of these gases ends.²

A useful and remarkably simple correlation for the Prandtl number has been proposed by van den Oord and Korving.¹⁸ By considering the total heat flux rather than its separate translational and internal components, a procedure that is mathematically equivalent to a simple linear transformation of the basis functions used to solve the Boltzmann equation, they obtained an alternative expression for λ in which a rather complicated term turns out to be small enough to be neglected in many cases. (Parenthetically, we note that this omission is equivalent to assuming a relation between D_{rot} and Z_{rot} .)¹ Further simplification was then achieved by recourse to some approximate relations among cross sections (including relations equivalent to the expression $Z_{\text{elec}}, Z_{\text{vib}} \gg Z_{\text{rot}}$); the final result, given in terms of the Prandtl number, is as follows:

$$Pr \approx \frac{2}{3} \left(1 + \frac{4}{3\pi} \frac{C_{\text{rot}}}{R} \right). \quad (3)$$

The results of this approximate formula are also presented in the deviation plots of Figs. D1–D9. Its accuracy (except for SF_6) and simplicity are such that it might often be preferable to the more accurate, but more complicated, results of the present correlation. The needed values of Z_{rot} can be calculated from Eq. (C4), with the values of Z_{rot}^∞ and ϵ/k given in Tables B3 and B4. However, Eq. (3) is very inaccurate for SF_6 (deviations up to 25%), perhaps because such a large fraction of the internal energy is carried by the vibrational degrees of freedom.

According to Eq. (3), the Prandtl number is a function of two reduced temperatures, kT/ϵ for Z_{rot} and T/θ_{rot} for C_{rot} , indexed with the parameter Z_{rot}^∞ . But θ_{rot} is so small compared to ϵ/k (see Tables B3 and B4) that for $T^* \gg 1$, C_{rot} has reached its high-temperature limiting value of R for linear molecules and $(3/2)R$ for nonlinear molecules. Consequently the Prandtl number, Pr , considered now as a function of $1/Z_{\text{rot}}$, should reduce to a straight line with an intercept of $Pr = 2/3$ and a slope proportional to C_{rot}/R . A plot of Pr vs $1/Z_{\text{rot}}$ for values calculated from the present correlation is shown in Fig.

D10 for the six linear molecules. According to Eq. (3) the values should fall on a straight line of slope $8/9\pi = 0.283$. The results follow this prediction only approximately, but a workable correlation nonetheless exists. It is perhaps worth noting that the largest deviations occur for O_2 and NO , the systems of lowest accuracy in the present correlation. The predictions of Eq. (3) are poorer for the nonlinear molecules CH_4 , CF_4 , and especially SF_6 .

Another way of presenting these results, in a form valid for both linear and nonlinear molecules, is to rearrange Eq. (3) as follows:

$$\left(\frac{3}{2}Pr - 1\right) \frac{Z_{rot}^{\infty} R}{C_{rot}} = \frac{4}{3\pi} \frac{Z_{rot}^{\infty}}{Z_{rot}} \approx f(T^*), \quad (4)$$

with a universal function $f(T^*)$ given, at least approximately, by the righthand side of Eq. (C4). The use of Eq. (3) or (4) may prove convenient when results of less than optimal accuracy are acceptable in particular applications.

6. Description of the Tables

The tables of numerical data are not meant to be exhaustive and have not been designed for linear interpolation. They are convenient extracts only, because the algorithm for each property can be programmed on a computer without difficulty on the basis of the information supplied here. They can be used for numerical checks of such programs.

The tables, one for each gas, are identical in their structure and give values of λ , C_p/R , Pr , and the thermal diffusivity κ , defined as

$$\kappa = \lambda / \rho c_p. \quad (5)$$

where c_p is the specific heat. SI units are used throughout, and κ is referred to a standard pressure of 1.013 25 bar (1 atm). Below 0 °C, the temperatures are listed in kelvins, above that in degrees Celsius in conformity with the common practice prevailing at this time.

7. Tables

TABLE 1. Thermal conductivity of N_2

T K or °C	λ mW/m K	C_p/R	Pr	$\kappa(1.013 \text{ bar})$ $10^{-4} \text{ m}^2/\text{s}$
100 K	8.62	3.500	0.8089	0.0243
150	13.55	3.501	0.7686	0.0573
200	18.02	3.501	0.7465	0.1016
250	22.10	3.501	0.7320	0.1557
300	25.88	3.503	0.7215	0.2188
0 °C	23.88	3.502	0.7268	0.1838
20	25.38	3.503	0.7228	0.2096
40	26.84	3.504	0.7192	0.2367
60	28.27	3.506	0.7159	0.2651
80	29.67	3.508	0.7129	0.2948
100	31.05	3.512	0.7102	0.3256
150	34.43	3.525	0.7043	0.4080
200	37.75	3.544	0.6993	0.4974
250	41.05	3.571	0.6952	0.5935
300	44.33	3.603	0.6917	0.6961
350	47.62	3.639	0.6887	0.8048
400	50.84	3.677	0.6870	0.9185
450	53.92	3.718	0.6872	1.0351
500	56.99	3.759	0.6875	1.1568
600	63.06	3.839	0.6879	1.4156
700	69.04	3.914	0.6883	1.6942
800	74.87	3.981	0.6885	1.9918
900	80.57	4.041	0.6886	2.3085
1000	86.15	4.094	0.6887	2.6444
1500	112.55	4.274	0.6885	4.6086
2000	137.11	4.371	0.6878	7.0364
2500	160.43	4.430	0.6871	9.9110
3000	182.89	4.469	0.6864	13.2185

TABLE 2. Thermal conductivity of O_2

T K or °C	λ mW/m K	C_p/R	Pr	$\kappa(1.013 \text{ bar})$ $10^{-4} \text{ m}^2/\text{s}$
150 K	13.36	3.501	0.7624	0.0565
200	18.07	3.503	0.7406	0.1018
250	22.45	3.512	0.7264	0.1577
300	26.64	3.534	0.7162	0.2232
0 °C	24.41	3.520	0.7213	0.1869
20	26.08	3.530	0.7174	0.2137
40	27.73	3.543	0.7140	0.2419
60	29.37	3.557	0.7109	0.2715
80	31.01	3.574	0.7082	0.3023
100	32.64	3.593	0.7057	0.3345
150	36.70	3.647	0.7005	0.4203
200	40.75	3.706	0.6963	0.5133
250	44.76	3.768	0.6930	0.6134
300	48.73	3.828	0.6902	0.7200
350	52.57	3.886	0.6886	0.8321
400	56.19	3.940	0.6892	0.9475
450	59.73	3.989	0.6897	1.0685
500	63.19	4.034	0.6902	1.1950
600	69.88	4.113	0.6908	1.4640
700	76.28	4.178	0.6911	1.7536
800	82.38	4.228	0.6912	2.0634
900	88.45	4.281	0.6913	2.3922
1000	94.20	4.319	0.6912	2.7402
1500	121.96	4.479	0.6885	4.7650
2000	149.08	4.619	0.6852	7.2403
2500	175.85	4.751	0.6829	10.1295
3000	201.98	4.867	0.6813	13.4070

TABLE 3. Thermal conductivity of NO

T K or °C	λ mW/m K	C_p/R	Pr	$\kappa(1.013 \text{ bar})$ $10^{-4} \text{ m}^2/\text{s}$
150 K	13.23	3.746	0.8053	0.0523
200	17.55	3.659	0.7808	0.0947
250	21.56	3.612	0.7639	0.1473
300	25.37	3.589	0.7513	0.2093
0 °C	23.34	3.599	0.7576	0.1749
20	24.86	3.591	0.7529	0.2002
40	26.34	3.587	0.7485	0.2270
60	27.82	3.586	0.7446	0.2551
80	29.28	3.587	0.7410	0.2844
100	30.73	3.592	0.7378	0.3151
150	34.35	3.613	0.7307	0.3970
200	37.95	3.646	0.7250	0.4861
250	41.56	3.686	0.7202	0.5821
300	45.16	3.732	0.7162	0.6846
350	48.75	3.779	0.7128	0.7934
400	52.32	3.827	0.7098	0.9082
450	55.85	3.873	0.7072	1.0290
500	59.33	3.918	0.7049	1.1555
600	66.15	4.000	0.7009	1.4253
700	72.76	4.070	0.6974	1.7168
800	79.16	4.131	0.6944	2.0294
900	85.27	4.182	0.6923	2.3607
1000	90.95	4.226	0.6922	2.7043
1500	117.61	4.368	0.6887	4.7113
2000	142.55	4.444	0.6835	7.1968
2500	166.18	4.490	0.6794	10.1295
3000	188.79	4.523	0.6765	13.4842

TABLE 4. Thermal conductivity of CO

T K or °C	λ mW/m K	C_p/R	Pr	$\kappa(1.013 \text{ bar})$ $10^{-4} \text{ m}^2/\text{s}$
100 K	8.19	3.500	0.8505	0.0231
150	13.01	3.501	0.8008	0.0550
200	17.38	3.501	0.7739	0.0980
250	21.38	3.502	0.7566	0.1507
300	25.11	3.505	0.7442	0.2121
0 °C	23.14	3.503	0.7504	0.1781
20	24.61	3.504	0.7457	0.2032
40	26.05	3.507	0.7415	0.2296
60	27.47	3.510	0.7377	0.2573
80	28.86	3.514	0.7342	0.2862
100	30.23	3.519	0.7311	0.3163
150	33.62	3.539	0.7243	0.3967
200	36.96	3.566	0.7186	0.4840
250	40.29	3.600	0.7140	0.5779
300	43.62	3.639	0.7100	0.6782
350	46.95	3.681	0.7066	0.7845
400	50.28	3.725	0.7037	0.8967
450	53.59	3.770	0.7011	1.0146
500	56.88	3.813	0.6988	1.1381
600	63.38	3.897	0.6949	1.4016
700	69.73	3.972	0.6915	1.6863
800	75.79	4.038	0.6898	1.9880
900	81.52	4.095	0.6898	2.3046
1000	87.10	4.145	0.6898	2.6403
1500	113.43	4.311	0.6891	4.6043
2000	137.90	4.399	0.6882	7.0322
2500	161.17	4.452	0.6874	9.9070
3000	183.61	4.488	0.6866	13.2146

TABLE 5. Thermal conductivity of CO₂

T K or °C	λ mW/m K	C_p/R	Pr	$\kappa(1.013 \text{ bar})$ $10^{-4} \text{ m}^2/\text{s}$
250 K	12.76	4.188	0.7754	0.0751
300	16.79	4.475	0.7592	0.1111
0 °C	14.60	4.324	0.7669	0.0911
20	16.23	4.437	0.7610	0.1058
40	17.87	4.546	0.7560	0.1215
60	19.52	4.651	0.7519	0.1380
80	21.18	4.751	0.7483	0.1554
100	22.84	4.847	0.7453	0.1736
150	27.00	5.068	0.7394	0.2225
200	31.12	5.266	0.7351	0.2760
250	35.20	5.444	0.7319	0.3339
300	39.23	5.606	0.7295	0.3959
350	43.20	5.753	0.7275	0.4619
400	47.11	5.886	0.7258	0.5317
450	50.72	5.981	0.7244	0.6053
500	54.61	6.107	0.7232	0.6823
600	62.23	6.333	0.7213	0.8468
700	69.24	6.491	0.7195	1.0246
800	76.08	6.631	0.7180	1.2151
900	82.64	6.748	0.7166	1.4180
1000	88.99	6.848	0.7153	1.6328
1500	117.17	7.168	0.7132	2.8603
2000	141.72	7.340	0.7124	4.3316
2500	164.19	7.446	0.7111	6.0347
3000	185.16	7.523	0.7102	7.9508

TABLE 6. Thermal conductivity of N₂O

T K or °C	λ mW/m K	C_p/R	Pr	$\kappa(1.013 \text{ bar})$ $10^{-4} \text{ m}^2/\text{s}$
300 K	17.47	4.655	0.7529	0.1112
0 °C	15.19	4.503	0.7600	0.0909
20	16.89	4.617	0.7546	0.1058
40	18.60	4.725	0.7500	0.1217
60	20.32	4.827	0.7462	0.1384
80	22.04	4.924	0.7430	0.1560
100	23.76	5.016	0.7403	0.1745
150	28.06	5.228	0.7349	0.2241
200	32.32	5.418	0.7311	0.2786
250	36.54	5.588	0.7282	0.3376
300	40.70	5.743	0.7259	0.4009
350	44.79	5.883	0.7242	0.4683
400	48.82	6.010	0.7227	0.5397
450	52.77	6.126	0.7214	0.6148
500	56.65	6.231	0.7204	0.6937
600	64.17	6.413	0.7185	0.8622
700	71.37	6.563	0.7170	1.0445
800	78.28	6.687	0.7156	1.2398
900	84.92	6.791	0.7142	1.4479
1000	91.31	6.877	0.7130	1.6683
1500	119.23	7.145	0.7131	2.9201
2000	143.50	7.274	0.7125	4.4254
2500	165.52	7.345	0.7113	6.1679
3000	185.87	7.387	0.7103	8.1280

TABLE 7. Thermal conductivity of CH₄

<i>T</i> K or °C	λ mW/m K	C_p/R	<i>Pr</i>	$\kappa(1.013 \text{ bar})$ $10^{-4} \text{ m}^2/\text{s}$
200 K	21.53	4.031	0.7447	0.1054
250	27.91	4.122	0.7270	0.1671
300	34.89	4.303	0.7152	0.2401
0 °C	31.05	4.194	0.7209	0.1996
20	33.89	4.273	0.7165	0.2295
40	36.86	4.365	0.7128	0.2610
60	39.96	4.469	0.7097	0.2940
80	43.21	4.584	0.7072	0.3285
100	46.58	4.708	0.7051	0.3644
150	55.41	5.043	0.7029	0.4589
200	64.48	5.399	0.7060	0.5576
250	74.02	5.762	0.7088	0.6633
300	83.94	6.123	0.7113	0.7755
350	94.15	6.476	0.7135	0.8941
400	104.59	6.820	0.7154	1.0189
450	115.21	7.152	0.7170	1.1497
500	125.96	7.472	0.7184	1.2863
600	147.71	8.072	0.7206	1.5769
700	169.58	8.619	0.7222	1.8897
800	191.35	9.112	0.7232	2.2240
900	212.87	9.555	0.7240	2.5793
1000	234.04	9.952	0.7244	2.9550
1500	333.66	11.389	0.7240	5.1267
2000	424.87	12.257	0.7204	7.7761
2500	510.39	12.841	0.7161	10.8782
3000	591.77	13.277	0.7126	14.3983

TABLE 8. Thermal conductivity of CF₄

<i>T</i> K or °C	λ mW/m K	C_p/R	<i>Pr</i>	$\kappa(1.013 \text{ bar})$ $10^{-4} \text{ m}^2/\text{s}$
200 K	8.09	5.697	0.8016	0.0280
250	11.87	6.570	0.7783	0.0446
300	15.92	7.371	0.7657	0.0639
0 °C	13.72	6.951	0.7716	0.0532
20	15.36	7.266	0.7670	0.0611
40	17.01	7.567	0.7634	0.0695
60	18.68	7.854	0.7603	0.0782
80	20.36	8.126	0.7579	0.0873
100	22.03	8.384	0.7558	0.0968
150	26.21	8.967	0.7518	0.1221
200	30.31	9.468	0.7489	0.1495
250	34.30	9.897	0.7468	0.1789
300	38.16	10.263	0.7450	0.2103
350	41.90	10.576	0.7435	0.2436
400	45.50	10.843	0.7422	0.2788
450	48.98	11.071	0.7409	0.3157
500	52.34	11.268	0.7398	0.3544
600	58.75	11.586	0.7376	0.4369
700	64.78	11.828	0.7356	0.5260
800	70.51	12.014	0.7336	0.6216
900	75.97	12.161	0.7317	0.7233
1000	81.22	12.278	0.7299	0.8311
1500	105.09	12.613	0.7212	1.4580
2000	136.98	12.761	0.6620	2.4081
2500	178.08	12.838	0.5897	3.7964
3000	226.67	12.883	0.5251	5.6835

TABLE 9. Thermal conductivity of SF₆

<i>T</i> K or °C	λ mW/m K	C_p/R	Pr	$\kappa(1.013 \text{ bar})$ $10^{-4} \text{ m}^2/\text{s}$
250 K	8.23	10.181	0.9019	0.0199
300	12.97	11.758	0.7894	0.0327
0 °C	10.50	10.950	0.8296	0.0259
20	12.35	11.561	0.7972	0.0309
40	14.12	12.121	0.7780	0.0360
60	15.64	12.633	0.7751	0.0407
80	17.14	13.101	0.7728	0.0456
100	18.64	13.526	0.7710	0.0507
150	22.26	14.432	0.7678	0.0644
200	25.73	15.150	0.7658	0.0793
250	29.04	15.723	0.7644	0.0953
300	32.18	16.185	0.7633	0.1125
350	35.18	16.560	0.7625	0.1307
400	38.05	16.868	0.7617	0.1499
450	40.80	17.123	0.7611	0.1701
500	43.45	17.336	0.7604	0.1912
600	48.47	17.669	0.7592	0.2364
700	53.18	17.913	0.7579	0.2851
800	57.64	18.097	0.7567	0.3373
900	61.90	18.238	0.7555	0.3929
1000	65.98	18.349	0.7542	0.4518
1500	84.52	18.658	0.7481	0.7927
2000	101.06	18.790	0.7424	1.2066
2500	116.32	18.858	0.7373	1.6881
3000	130.55	18.898	0.7330	2.2315

8. Acknowledgments

This work was supported in part under NSF Grants CHE 85-09416 and CHE 88-19370, and in part by CONACYT (Mexico). We thank Professor W. A. Wakeham of Imperial College for his helpful cooperation in exchanging information and ideas. The correlation work has been carried out under the auspices of the Subcommittee on Transport Properties of Commission I.2 of the International Union of Pure and Applied Chemistry.

9. References to Introductory Text

- ¹F. J. Uribe, E. A. Mason, and J. Kestin, *Physica* **A156**, 467 (1989).
- ²A. Boushehri, J. Bzowski, J. Kestin, and E. A. Mason, *J. Phys. Chem. Ref. Data* **16**, 445 (1987).
- ³E. A. Mason and L. Monchick, *J. Chem. Phys.* **36**, 1622 (1962).
- ⁴L. Monchick, A. N. G. Pereira, and E. A. Mason, *J. Chem. Phys.* **42**, 3241 (1965).
- ⁵J. D. Lambert, *Vibrational and Rotational Relaxation in Gases* (Clarendon, Oxford, 1977).
- ⁶H. O. Kneser, H.-J. Bauer, and H. Kosche, *J. Acoust. Soc. Am.* **41**, 1029 (1967).
- ⁷JANAF Thermochemical Tables, U. S. National Bureau of Standards NSRDS-NBS37 (Washington, DC, 2nd ed., 1971).

^{7b}R. A. McDowell and F. H. Kruse, *J. Chem. Eng. Data* **7**, 547 (1963). CH₄.

⁸J. G. Parker, *Phys. Fluids* **2**, 449 (1959).

⁹C. A. Brau and R. M. Jonkman, *J. Chem. Phys.* **52**, 477 (1970).

¹⁰E. R. Cohen and B. N. Taylor, *J. Phys. Chem. Ref. Data* **17**, 1795 (1988).

¹¹J. R. DeLaeter, *J. Phys. Chem. Ref. Data* **17**, 1791 (1988).

¹²G. C. Maitland, M. Mustafa, M. Ross, R. D. Trengove, W. A. Wakeham, and M. Zalaf, *Int. J. Thermophys.* **7**, 245 (1986).

¹³J. Millat and W. A. Wakeham, *J. Phys. Chem. Ref. Data* **18**, 565 (1989).

¹⁴J. Millat, V. Vesovic, and W. A. Wakeham, *Physica* **A148**, 153 (1988).

¹⁵H. J. M. Hanley and J. F. Ely, *J. Phys. Chem. Ref. Data* **2**, 735 (1973).

¹⁶H. J. M. Hanley, W. M. Haynes, and R. D. McCarty, *J. Phys. Chem. Ref. Data* **6**, 597 (1977).

¹⁷K. Stephan, R. Krauss, and A. Laesecke, *J. Phys. Chem. Ref. Data* **16**, 993 (1987).

¹⁸R. J. van den Oord and J. Korving, *J. Chem. Phys.* **89**, 4333 (1988).

Appendix A

General Formulas

$$\lambda = \lambda_{\text{tr}} + \lambda_{\text{rot}} + \lambda_{\text{vib}} + \lambda_{\text{elec}} \quad (\text{A1})$$

$$\frac{M\lambda_{\text{tr}}}{\eta R} = \frac{5}{2} \left(\frac{3}{2} - \Delta_{\text{rot}} \right) (1 + \Delta_{\text{spin}}), \quad (\text{A2})$$

$$\frac{M\lambda_{\text{rot}}}{\eta R} = \frac{\rho D_{\text{rot}}}{\eta} \left(\frac{C_{\text{rot}}}{R} + \Delta_{\text{rot}} \right) \left(\frac{1 + \Delta_{\text{spin}}}{1 + \Delta_{\text{ex}}^{\mu\mu} + \Delta_{\text{ex}}^{\mu\theta} + \Delta_{\text{ex}}^{\theta\theta}} \right), \quad (\text{A3})$$

$$\frac{M\lambda_{\text{vib}}}{\eta R} = \frac{\rho D_{\text{vib}}}{\eta} \frac{C_{\text{vib}}}{R} \approx \frac{6}{5} A^* \frac{C_{\text{vib}}}{R}, \quad (\text{A4})$$

$$\frac{M\lambda_{\text{elec}}}{\eta R} = \frac{\rho D_{\text{elec}}}{\eta} \frac{C_{\text{elec}}}{R} \approx \frac{6}{5} A^* \frac{C_{\text{elec}}}{R}, \quad (\text{A5})$$

where C_{rot} , C_{vib} , and C_{elec} are the molar heat capacities.

$$\Delta_{\text{rot}} = \frac{2}{\pi Z_{\text{rot}}} \frac{C_{\text{rot}}}{R} \left(\frac{5}{2} - \frac{D_{\text{rot}}}{\eta} \right) \left[1 + \frac{2}{\pi Z_{\text{rot}}} \left(\frac{5}{3} \frac{C_{\text{rot}}}{R} + \frac{\rho D_{\text{rot}}}{\eta} \right) \right]^{-1}, \quad (\text{A6})$$

$$\Delta_{\text{spin}} = -\frac{5}{3} \left(\frac{\Delta\lambda_{\parallel}}{\lambda} \right)_{\text{sat}} \approx \frac{C_{\text{spin}} \left(\frac{5}{2} + \frac{C_{\text{rot}}}{R} \right) \frac{\rho D_{\text{rot}}}{\eta}}{\left(1 + \frac{8}{15\pi Z_{\text{rot}}} \frac{C_{\text{rot}}}{R} \right) \frac{\rho D_{\text{rot}}}{\eta} + \frac{3}{5} \frac{C_{\text{rot}}}{R}}, \quad (\text{A7})$$

where $(\Delta\lambda_{\parallel}/\lambda)_{\text{sat}}$ sat the saturation (i.e., high-field) value of the fractional change in λ when a magnetic field is applied parallel to the temperature gradient. It is an experimentally known quantity, at least at 300 K. The dimensionless constant C_{spin} is needed to calculate the temperature dependence of Δ_{spin} ; it is given in Table B4.

$$\Delta_{\text{ex}}^{\mu\mu} = 0.44 g^{\mu\mu} \left(\frac{3\pi^2}{2} \right) \left(\frac{\pi}{2} \right)^{1/2} \frac{\mu^2}{\hbar} \frac{\eta}{kT} \frac{\rho D_{\text{rot}}}{\eta} \left(\frac{\theta_{\text{rot}}}{T} \right)^{3/2}, \quad (\text{A8})$$

$$\Delta_{\text{ex}}^{\mu\ominus} = 0.51g^{\mu\ominus} \left(\frac{56\pi^2}{45} \left(\frac{3}{5} \right)^{1/2} \left(\frac{\pi^2}{6} \right)^{1/3} \left(\frac{\mu|\Theta|}{\hbar} \right)^{2/3} \left(\frac{RT}{M} \right)^{1/6} \right. \\ \left. \times \frac{\eta}{kT} \frac{\rho D_{\text{rot}}}{\eta} \left(\frac{\theta_{\text{rot}}}{T} \right)^{3/2}, \quad (\text{A9})$$

$$\Delta_{\text{ex}}^{\ominus\ominus} = 1.31g^{\ominus\ominus} \left(\frac{7\pi^{3/2}}{2} \right) \Gamma\left(\frac{7}{4}\right) \left(\frac{\Theta^2}{\hbar} \right)^{1/2} \\ \times \left(\frac{RT}{M} \right)^{1/4} \frac{\eta}{kT} \frac{\rho D_{\text{rot}}}{\eta} \left(\frac{\theta_{\text{rot}}}{T} \right)^{3/2}, \quad (\text{A10})$$

where $g^{\mu\mu}$, $g^{\mu\ominus}$, and $g^{\ominus\ominus}$ are temperature-dependent dimensionless factors of order unity that are given in Appendix C.

The term Δ_{spin} amounts to less than a 1.5% correction, and for all practical purposes is temperature independent, for all the systems considered here.¹ It would be larger for more anisotropic molecules. The Δ_{ex} terms give less than 1% total correction for the present systems, but are much larger for strongly polar molecules with small moments of inertia (e.g., HCl, NH₃, H₂O).^{1,3}

For completeness, the expression for the viscosity is,

$$\eta = \frac{5}{16} \left(\frac{mkT}{\pi} \right)^{1/2} \frac{f_{\eta}}{\sigma^2 \Omega^{(2,2)*}}, \quad (\text{A11})$$

where the functional $\Omega^{(2,2)*}$ is given in Appendix C, and

$$f_{\eta} = 1 + (3/196)(8E^* - 7)^2, \quad (\text{A12})$$

$$E^* = \frac{\Omega^{(2,3)*}}{\Omega^{(2,2)*}} = 1 + \frac{T^*}{4} \frac{d \ln \Omega^{(2,2)*}}{dT^*}. \quad (\text{A13})$$

Values of the parameter σ are tabulated in Ref. 2, as are numerical values of η .

Appendix B

Material and Physical Constants Including Scaling Factors

TABLE B1. Universal constants^a

Boltzmann constant	$k = 1.380658 \times 10^{-23} \text{ J K}^{-1}$
Avogadro constant	$N_A = 6.0221367 \times 10^{23} \text{ mol}^{-1}$
Universal gas constant	$R = 8.314 510 \text{ J mol}^{-1} \text{ K}^{-1}$
Planck constant	$\hbar = h/2\pi = 1.054 572 66 \times 10^{-34} \text{ J s}$

^aRef. 10.

TABLE B2. Molecular Weights^a (standard isotopic composition)

N ₂	28.0135
O ₂	31.9988
NO	30.0061
CO	28.010
CO ₂	44.010
N ₂ O	44.0129
CH ₄	16.043
CF ₄	88.005
SF ₆	146.056

^aRef. 11.

TABLE B3. Effective spherical scaling parameters, ϵ/k for low temperatures and $V_0^* = V_0/\epsilon$ and ρ^* for high temperatures^a

	$\epsilon/k(\text{K})$	V_0^*	ρ^*
N ₂	98.4	5.308×10^4	0.1080
O ₂	121.1	1.322×10^6	0.0745
NO	125.0	2.145×10^5	0.0883
CO	98.4	5.308×10^4	0.1080
CO ₂	245.3	2.800×10^6	0.0720
N ₂ O	266.8	2.600×10^6	0.0730
CH ₄	161.4	3.066×10^6	0.0698
CF ₄	156.5	1.460×10^{19}	0.0200
SF ₆	207.7	4.067×10^8	0.0500

^aRef. 2.

TABLE B4. Material parameters for the calculation of D_{rot} and λ

	Z_{rot}^a	$10^3 C_{\text{spin}}^c$	$ \Theta ^j$ (10^{-18} esu)	μ^i (10^{-26} esu)	θ_{rot}^f (K)
N ₂	29.5	5.7	0	1.4 ^k	2.88
O ₂	36 ^b	6.1	0	0.39	2.07
NO	24 ^c	(5.9) ^f	0.153	1.8	2.45
CO	22.2	6.1	0.112	2.5	2.77
CO ₂	32.0	6.3 ^g	0	4.3	0.561
N ₂ O	36.2	(6.3) ^h	0.167	3.0	0.603
CH ₄	61.5	1.2	0	0	
CF ₄	24.9	2.2	0	0	
SF ₆	12.6 ^d	1.4	0	0	

^aRef. 1, unless otherwise noted.

^bE. H. Carnevale, C. Carey, and G. Larson, *J. Chem. Phys.* **47**, 2829 (1967) give $Z_{\text{rot}} = 4.5$ at 300 K; our value is 6.0.

^cAssumed to be similar to N₂, O₂, and CO. This gives $Z_{\text{rot}} = 3.9$ at 300 K, compared to the value of 2.9 from Ref. 6.

^dC. J. Jameson and A. K. Jameson, *J. Chem. Phys.* **88**, 7448 (1988) give results corresponding to $Z_{\text{rot}} = 13.8$.

^eFrom the Senftleben-Beenakker effect measurements of L. J. F. Hermans, J. M. Koks, A. F. Hengeveld, and H. F. P. Knaap, *Physica* **50**, 410 (1970), unless otherwise noted.

^fNot measured; assumed to be similar to N₂ and O₂, in accordance with the measurements of J. Korving, W. I. Honeywell, T. K. Bose, and J. J. M. Beenakker, *Physica* **36**, 198 (1967).

^gB. J. Thijsse, W. A. P. Denissen, L. J. F. Hermans, H. F. P. Knaap, and J. J. M. Beenakker, *Physica* **97A**, 467 (1979).

^hNot measured; assumed to be the same as for CO₂.

ⁱR. D. Nelson, Jr., D. R. Lide, Jr., and A. A. Maryott, U. S. National Bureau of Standards NSRDS-NBS 10 (Washington, DC, 1967).

¹D. E. Stogryn and A. P. Stogryn, *Mol. Phys.* **11**, 371 (1966), unless otherwise noted.
²A. D. Buckingham, R. L. Disch, and D. A. Dunmur, *J. Am. Chem. Soc.* **90**, 3104 (1968). See comments by F. P. Billingsley II and M. Krauss, *J. Chem. Phys.* **60**, 2767 (1974).
³D. A. McQuarrie, *Statistical Mechanics* (Harper and Row, NY, 1967), pp. 95, 132.

Appendix C

Correlation Equations for Functionals

$$A^* = \Omega^{(2,2)*} / \Omega^{(1,1)*} \quad (C1)$$

$\Omega^{(2,2)*}$:

$1 < T^* < 10$,

$$\Omega^{(2,2)*} = \exp [0.46641 - 0.56991(\ln T^*) + 0.19591(\ln T^*)^2 - 0.03879(\ln T^*)^3 + 0.00259(\ln T^*)^4]. \quad (C2a)$$

$T^* > 10$,

$$\Omega^{(2,2)*} = (\rho^*)^2 \alpha^2 [1.04 + a_1(\ln T^*)^{-1} + a_2(\ln T^*)^{-2} + a_3(\ln T^*)^{-3} + a_4(\ln T^*)^{-4}], \quad (C2b)$$

where

$$a_1 = 0$$

$$a_2 = -33.0838 + (\alpha_{10}\rho^*)^{-2}[20.0862 + (72.1059/\alpha_{10}) + (8.27648/\alpha_{10})^2],$$

$$a_3 = 1.01571 - (\alpha_{10}\rho^*)^{-2}[56.4472 + (286.393/\alpha_{10}) + (17.7610/\alpha_{10})^2],$$

$$a_4 = -87.7036 + (\alpha_{10}\rho^*)^{-2}[46.3130 + (277.146/\alpha_{10}) + (19.0573/\alpha_{10})^2],$$

in which $\alpha_{10} = \ln(V_0^*/10)$ is the value of $\alpha = \ln(V_0^*/T^*)$ at the matching point of $T^* = 10$. These expressions are identical to those of Ref. 2.

$\Omega^{(1,1)*}$:

$1 < T^* < 10$,

$$\Omega^{(1,1)*} = \exp[0.295402 - 0.510069 \ln T^* + 0.189395(\ln T^*)^2 - 0.045427(\ln T^*)^3 + 0.0037928(\ln T^*)^4]. \quad (C3a)$$

$T^* \geq 10$,

$$\Omega^{(1,1)*} = (\rho^*)^2 \alpha^2 [0.89 + b_2(T^*)^{-2} + b_4(T^*)^{-4} + b_6(T^*)^{-6}], \quad (C3b)$$

where

$$b_2 = -267.00 + (\alpha_{10}\rho^*)^{-2} [201.570 + (174.672/\alpha_{10}) + (7.36916/\alpha_{10})^2],$$

$$b_4 = 26700 - (\alpha_{10}\rho^*)^{-2} [19.2265 + (27.6938/\alpha_{10}) + (3.29559/\alpha_{10})^2] \times 10^3,$$

$$b_6 = -8.90 \times 10^5 + (\alpha_{10}\rho^*)^{-2} [6.31013 + (10.2266/\alpha_{10}) + (2.33033/\alpha_{10})^2] \times 10^5,$$

in which $\alpha_{10} = \ln(V_0^*/10)$ is the value of $\alpha = \ln(V_0^*/T^*)$ at the matching point of $T^* = 10$. These expressions are identical to those of Ref. 2.

$$\frac{Z_{rot}^\infty}{Z_{rot}} = 1 + \frac{c_1}{(T^*)^{1/2}} + \frac{c_2}{T^*} + \frac{c_3}{(T^*)^{3/2}}, \quad (C4)$$

where

$$c_1 = \pi^{3/2}/2 = 2.78,$$

$$c_2 = 2 + \pi^2/4 = 4.47,$$

$$c_3 = \pi^{3/2} = 5.57.$$

$\rho D_{rot}/\eta$:

$T^* < T_{cross}^*$,

$$\frac{\rho D_{rot}}{\eta} = (Z_{rot}^\infty)^{1/4} \left(1.122 + \frac{4.552}{T^2} \right) \frac{Z_{rot}}{Z_{rot}^\infty}. \quad (C5a)$$

$T^* > T_{cross}^*$

$$\frac{\rho D_{rot}}{\eta} = \frac{6}{5} A^* \left[1 + \frac{0.27}{Z_{rot}^\infty} - \frac{0.44}{(Z_{rot}^\infty)^2} - \frac{0.90}{(Z_{rot}^\infty)^3} \right]. \quad (C5b)$$

Values of T_{cross}^* are given in Table C1.

TABLE C1. Values of T_{cross}^* for switching from Eq. (C5a) to Eq. (C5b) for $\rho D_{\text{rot}}/\eta$

	T_{cross}^*
N ₂	6.70
O ₂	5.02
NO	9.22
CO	10.48
CO ₂	5.94
N ₂ O	4.99
CH ₄	2.55
CF ₄	8.68
SF ₆	28.57

$$g^{\mu\mu} = e^{-2\theta_{\text{rot}}/3T} \left(1 - \frac{\theta_{\text{rot}}}{3T} + \dots \right), \quad (\text{C6a})$$

$$g^{\mu\Theta} = e^{-17\theta_{\text{rot}}/12T} \left(1 - \frac{5\theta_{\text{rot}}}{6T} + \dots \right), \quad (\text{C6b})$$

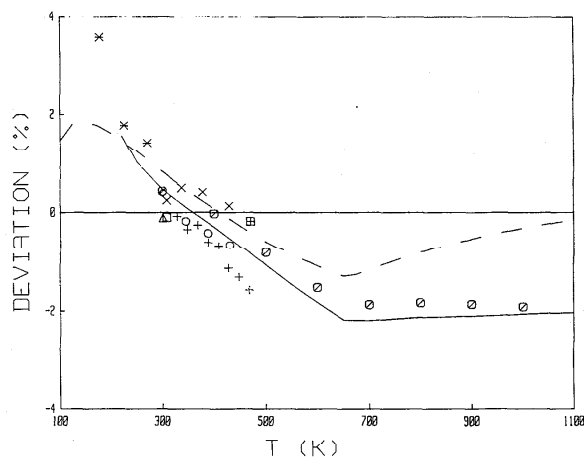
$$g^{\Theta\Theta} = e^{-13\theta_{\text{rot}}/6T} \left(1 - \frac{4\theta_{\text{rot}}}{3T} + \dots \right), \quad (\text{C6c})$$

More accurate numerical results for low T have been tabulated by C. Nyeland, E. A. Mason, and L. Monchick, J. Chem. Phys. **56**, 6180 (1972).

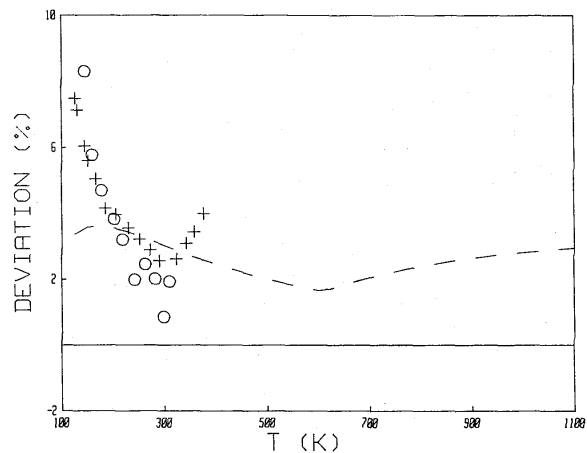
Appendix D

Deviation Plots

Note: the percentage deviation in the deviation plots refers to $100[\lambda(\text{meas}) - \lambda(\text{calc})]/\lambda(\text{calc})$.

FIG. D1. Deviation plot for the conductivity of N₂.

- | | |
|----------------------|--------------------|
| □ Ref. 1, PD | ⊠ Ref. 9, PD |
| ◇ Ref. 2, PD | ○ Ref. 10, PD |
| × Ref. 5, PD | * Ref. 15, PD |
| △ Ref. 8, PD | + Ref. 4, SD |
| ⊙ Ref. 17, correl. | — Ref. 18, correl. |
| - - Ref. 26, correl. | |

FIG. D2. Deviation plot for the conductivity of O₂.

- | | |
|----------------------|---------------|
| + Ref. 11, SD | ○ Ref. 20, SD |
| - - Ref. 26, correl. | |

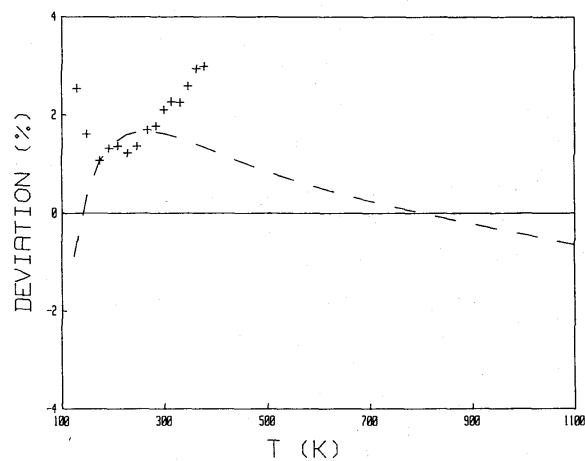


FIG. D3. Deviation plot for the conductivity of NO.

- | | |
|---------------|----------------------|
| + Ref. 11, SD | - - Ref. 26, correl. |
|---------------|----------------------|

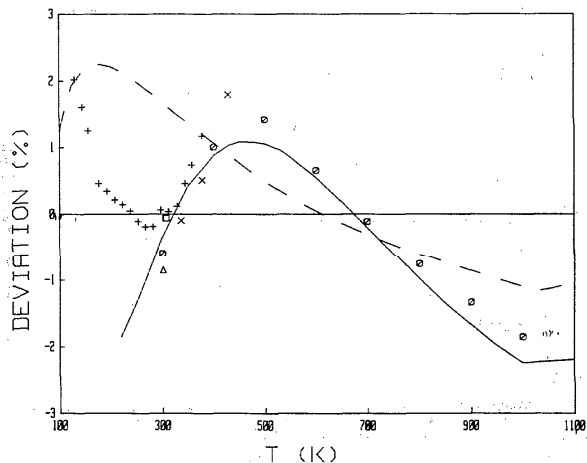


FIG. D4. Deviation plot for the conductivity of CO.

- Ref. 1, PD
- × Ref. 5, PD
- △ Ref. 8, PD
- + Ref. 11, SD
- ⊙ Ref. 17, correl.
- Ref. 18, correl.
- - - Ref. 26, correl.

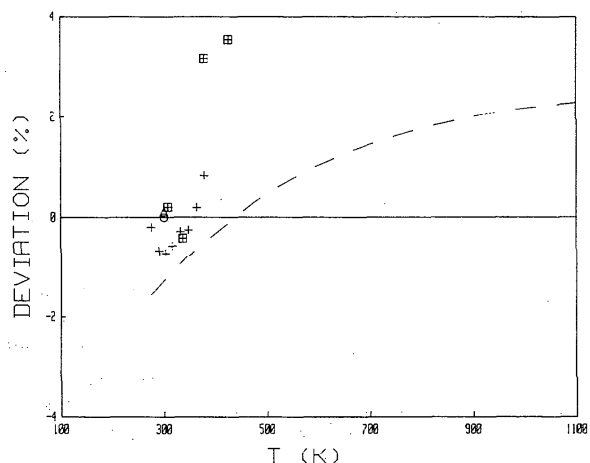


FIG. D6. Deviation plot for the conductivity of N₂O.

- Ref. 3, PD
- △ Ref. 8, PD
- ⊠ Ref. 14, PD
- + Ref. 11, SD
- - - Ref. 26, correl.

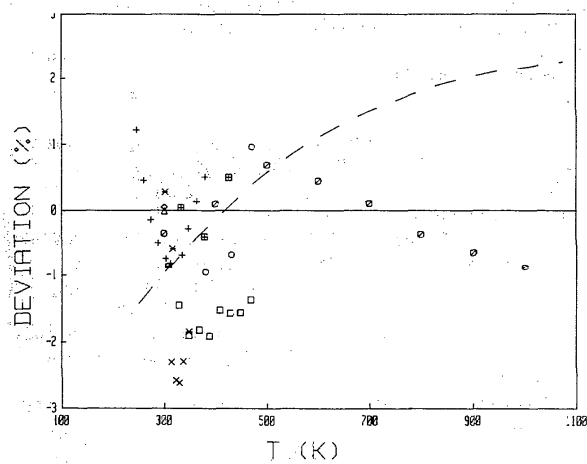


FIG. D5. Deviation plot for the conductivity of CO₂.

- ◇ Ref. 2, PD
- △ Ref. 8, PD
- Ref. 10, PD
- ⊕ Ref. 14, PD
- * Ref. 23, PD
- Ref. 4, SD
- + Ref. 11, SD
- × Ref. 25, SD
- ⊙ Ref. 17, correl.
- - - Ref. 26, correl.

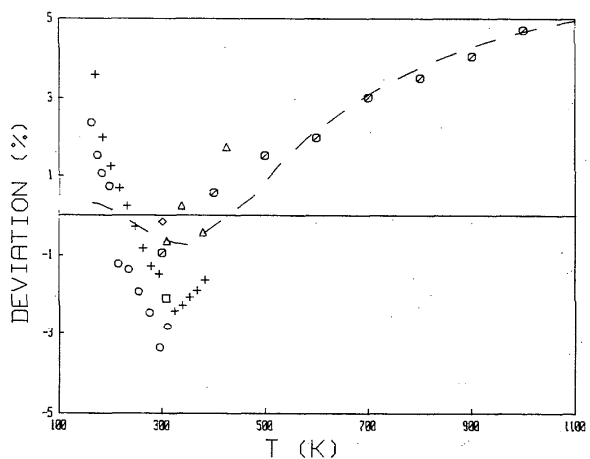


FIG. D7. Deviation plot for the conductivity of CH₄.

- Ref. 1, PD
- ◇ Ref. 2, PD
- △ Ref. 16, PD
- + Ref. 11, SD
- Ref. 21, SD
- ⊙ Ref. 17, correl.
- - - Ref. 26, correl.

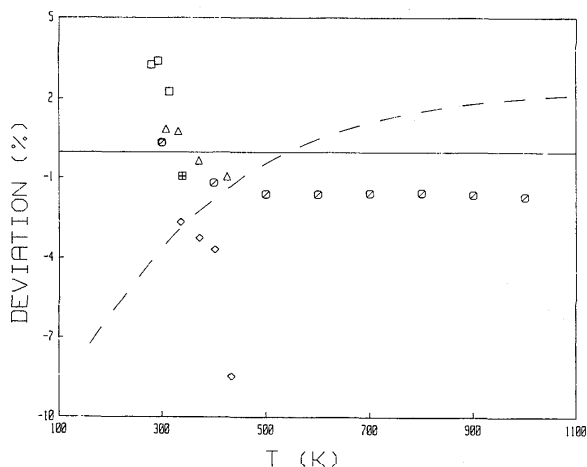
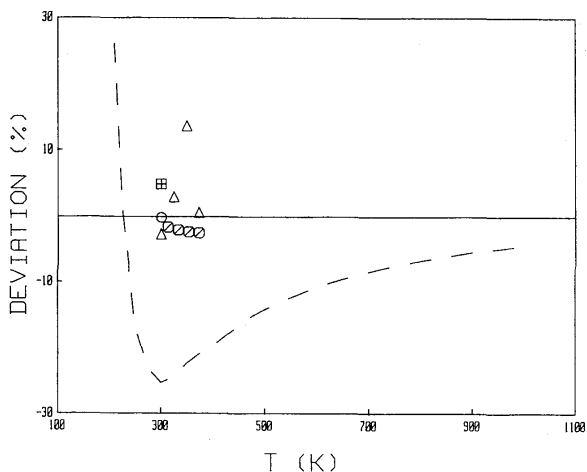
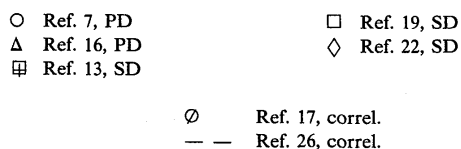
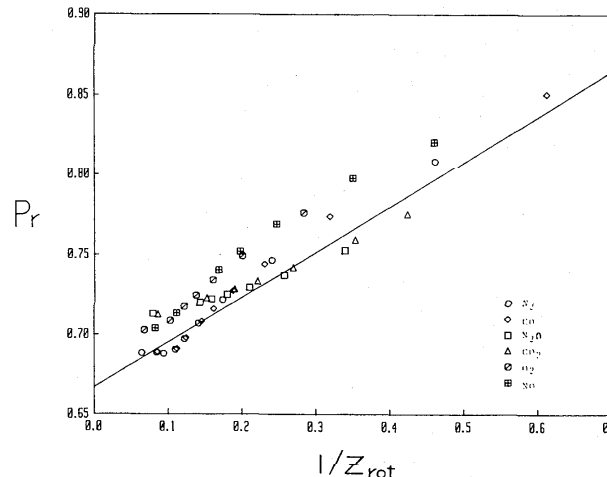
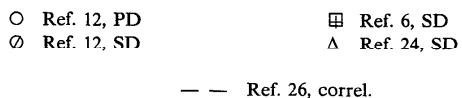
FIG. D8. Deviation plot for the conductivity of CF_4 .FIG. D9. Deviation plot for the conductivity of SF_6 .

FIG. D10. Correlation of the Prandtl number and rotational collision number according to Eq. (3).

Appendix E

References for Deviation Plots

- ¹M. J. Assael and W. A. Wakeham, *J. Chem. Soc. Faraday Trans. I* **77**, 697 (1981).
- ²A. A. Clifford, J. Kestin, and W. A. Wakeham, *Physica* **A97**, 287 (1979).
- ³R. Fleeter, J. Kestin, and W. A. Wakeham, *Physica* **A103**, 521 (1980).
- ⁴J. W. Haarman, *AIP Conf. Proc.* **11**, 193 (1973).
- ⁵E. N. Haran, G. C. Maitland, M. Mustafa, and W. A. Wakeham, *Ber. Bunsenges. Phys. Chem.* **87**, 657 (1983).
- ⁶L. J. F. Hermans, J. M. Koks, A. F. Hengeveld, and H. F. P. Knaap, *Physica* **50**, 410 (1970).
- ⁷N. Imaishi, J. Kestin, and R. Paul, *Int. J. Thermophys.* **6**, 3 (1985).
- ⁸N. Imaishi, J. Kestin, and W. A. Wakeham, *Physica* **A123**, 50 (1984).
- ⁹A. I. Johns, S. Rashid, L. Rowan, J. T. R. Watson, and A. A. Clifford, *Int. J. Thermophys.* **9**, 3 (1988).
- ¹⁰A. I. Johns, S. Rashid, J. T. R. Watson, and A. A. Clifford, *J. Chem. Soc. Faraday Trans. I* **82**, 2235 (1986).
- ¹¹H. L. Johnston and E. R. Grilly, *J. Chem. Phys.* **14**, 233 (1946).
- ¹²J. Kestin and N. Imaishi, *Int. J. Thermophys.* **6**, 107 (1985).
- ¹³J. D. Lambert, K. J. Cotton, M. W. Pailthorpe, A. M. Robinson, J. Scrivens, W. R. F. Vale, and R. M. Young, *Proc. Roy. Soc. London* **A231**, 280 (1955).
- ¹⁴J. Millat, M. Mustafa, M. Ross, W. A. Wakeham, and M. Zalaf, *Physica* **A145**, 461 (1987).
- ¹⁵J. Millat, M. J. Ross, and W. A. Wakeham, to be published.
- ¹⁶J. Millat, M. Ross, W. A. Wakeham, and M. Zalaf, *Physica* **A148**, 124 (1988).
- ¹⁷M. Millat, V. Vesovic, and W. A. Wakeham, *Physica* **148A**, 153 (1988).
- ¹⁸J. Millat and W. A. Wakeham, *J. Phys. Chem. Ref. Data* **18**, 565 (1989).
- ¹⁹S. Oshen, B. M. Rosenbaum, and G. Thodos, *J. Chem. Phys.* **46**, 2939 (1967).
- ²⁰H. M. Roder, *J. Res. NBS* **87**, 279 (1982).
- ²¹H. M. Roder, *Int. J. Thermophys.* **6**, 119 (1985).
- ²²B. M. Rosenbaum and G. Thodos, *Physica* **37**, 442 (1967).
- ²³A. C. Scott, A. I. Johns, J. T. R. Watson, and A. A. Clifford, *J. Chem. Soc. Faraday Trans. I* **79**, 733 (1983).
- ²⁴Y. Tanaka, M. Noguchi, H. Kubota, and T. Makita, *J. Chem. Eng. Japan* **12**, 171 (1979).
- ²⁵L. B. Thomas and R. C. Golike, *J. Chem. Phys.* **22**, 300 (1954).
- ²⁶R. J. van den Oord and J. Korving, *J. Chem. Phys.* **89**, 4333 (1988).